

M. GRAPINET¹
P. MATHEY^{1,✉}
S. ODOULOV²
D. RYTZ³

Semilinear coherent oscillator with reflection-type photorefractive gratings

¹ Laboratoire de Physique de l'Université de Bourgogne, UMR 5027 CNRS, 9 avenue Alain Savary, 21078 Dijon Cedex, France

² Institute of Physics, National Academy of Sciences, 03650, Kiev-39, Ukraine

³ Forschungsinstitut für mineralische und metallische Werkstoffe, Edelsteine Edelmetalle GmbH, 55743 Idar-Oberstein, Germany

Received: 3 September 2003

Published online: 28 October 2003 • © Springer-Verlag 2003

ABSTRACT The saturation intensity, oscillation spectrum, and temporal dynamics of oscillation are studied for a semilinear coherent oscillator with two counterpropagating pump waves and a photorefractive crystal with dominating reflection gratings. The instability of the single-frequency oscillation spectrum is revealed, similar to that known for an oscillator with dominating transmission gratings. The experimental manifestation of this transition in the output characteristics of the oscillator is favourably compared with numerical calculations.

PACS 42.65.Hw; 05.45.-a; 42.65.Pc; 42.65.Sf

1 Introduction

A semilinear coherent oscillator with two counterpropagating pump waves consists of a conventional mirror and a four-wave-mixing phase-conjugate mirror that ensures an amplified phase-conjugate reflectivity [1]. With a phase-conjugate mirror in a cavity such an oscillator allows for compensation of intracavity phase distortions [2], which makes it interesting for practical applications: with a conventional laser gain medium put inside the cavity the small divergence of the output oscillation wave should remain nearly unaffected by imperfect optical quality of the inserted gain medium [3]. It is attractive also as an example of a nonlinear device with rich temporal dynamics. For a multimode semilinear coherent oscillator, the transition from regular to chaotic behaviour was revealed, by controlling a cavity Fresnel number [4]. Recently, the instability of single-frequency operation was reported for a semilinear coherent oscillator with a single transverse mode [5, 6]. The analogy of coherent oscillation in

a semilinear cavity to a phase transition was found and a Curie–Weiss law for critical slowing down near the threshold of oscillation was revealed [7, 8].

In the present paper we describe the first (to our knowledge) implementation of a semilinear coherent oscillator with reflection-type photorefractive gratings. The output characteristics are measured and compared with the results of simulation. The coupling from reflection gratings is very seldom used in photorefractive coherent oscillators in spite of the fact that the gain can be rather high and the spatial overlap of the oscillation wave and pump waves can be much better than in oscillators based on transmission gratings [9–12].

It is shown that the threshold behaviour for the reflection-grating-based oscillator is identical to that of an oscillator with transmission gratings. The pump-ratio dependences of the oscillation intensity are shown to be strongly affected by the transition from single-frequency to two-frequency oscillation. This transition spreads the interval of pump ratios where oscillation occurs and results, for a certain set of param-

eters, in the increase of the oscillation efficiency. Both these effects are observed experimentally, explained qualitatively, and confirmed by calculations.

2 Experiment

A schematic representation of the experimental set-up is shown in Fig. 1. A cobalt-doped BaTiO₃ crystal (20 ppm in the melt) cut along crystallographic directions with dimensions $a_1 \times a_2 \times c = 3.7 \times 4 \times 6.1 \text{ mm}^3$ is used. An Ar⁺-laser beam (TEM₀₀, no etalon inside the cavity, wavelength $\lambda = 514 \text{ nm}$, 400-mW output power, polarised in the plane of the Fig. 1 drawing) is split to form two counterpropagating pump waves, 1 and 2. The path difference of the two pump waves of about 75 cm is large compared to the laser-beam coherence length (a few cm). A conventional cavity mirror M_c with 50-cm radius of curvature is placed at 38 cm from the sample. In such a way the path difference is reduced to zero for pump wave 1 and wave 4 that is reflected back to the sample by the mirror M_c. A small aperture (0.5 mm) is put inside the cavity at 5 cm from the conventional mirror. A Faraday rotator is placed at the Ar⁺-laser output mirror to prevent undesirable feedback to the pump laser from the coherent oscillator.

The sample is tilted so that pump waves 1 and 2 are inclined 191° and 11° with regard to the spontaneous polarisation axis (Z axis). The position of the conventional mirror ensures the angle 17° or 197° between the sample polar axis and oscillation waves 3 and 4, respectively. All values are given for angles inside the sample. This geometry, in accordance with the calculations of [9],

✉ Fax: +33-3/8039-5961, E-mail: pmathey@u-bourgogne.fr

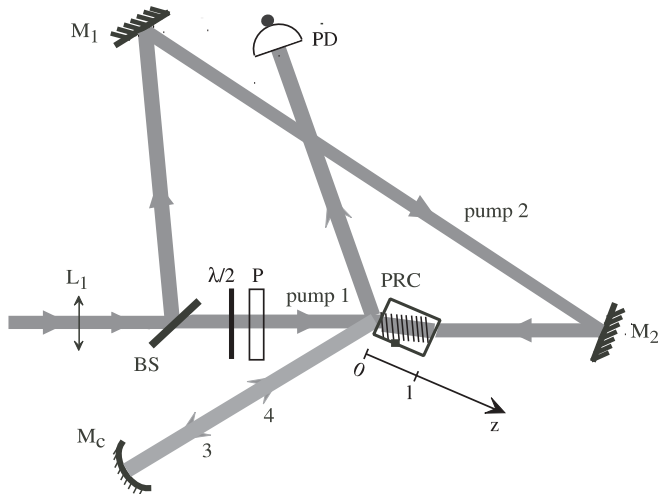


FIGURE 1 Experimental set-up with the photorefractive crystal PRC, beam splitter BS, mirrors M, photodetector PD, phase retarder $\lambda/2$, polariser P, and lens L_1

is close to be optimised for a largest possible gain from the reflection grating in BaTiO_3 . In our experiment a strong light-induced scattering was observed in this direction. The estimated coupling strength is not less than $\gamma\ell \approx 7$ for a reasonable effective trap density $N_{\text{eff}} \approx 10^{23} \text{ m}^{-3}$. Here γ is the coupling constant (see e.g. [4]) and ℓ is the crystal length along the c axis.

The pump waves are loosely focused inside the sample with a lens of 100-cm focal length. A half-wave phase retarder $\lambda/2$ and a polariser P allow for reduction of the pump 1 intensity keeping the intensity of pump 2 constant. The smallest pump-intensity ratio is $r = I_2(\ell)/I_1(0) \approx 20$, i.e. the total intensity of the two pump waves remains nearly constant when r is changing (it varies less than 5%).

The detector PD is used to measure the dynamics of the oscillation intensity. It collects the beam reflected from the sample face and therefore the signal measured is proportional to $I_3(0)$. Depending on the particular value of the pump ratio the oscillation dynamics at saturation is either smooth or features periodic variations, in a similar way as for a semilinear oscillator with transmission gratings [5, 6]. The periodic variation of the oscillation intensity in time proves the existence of two temporal frequencies in the oscillation spectrum; they can be extracted from the beat frequency.

From the oscillation dynamics measured at different intensities of pump 1 the pump-ratio dependences are plot-

ted for the oscillation intensity and the oscillation frequency. Figure 2 shows three representative pairs of dependences. For every pair (with identical symbols used, either filled dots, or triangles, or diamonds) the pump ratio is the only parameter that is changing. Different pairs are obtained after readjustment of pump waves inside the sample (which can affect, in principle, the coupling strength) and, more important, after readjustment of the aperture position inside the cavity (which affects considerably the efficient cavity losses).

A common feature of all three spectra is a supercritical bifurcation that

has already been observed for oscillators with transmission gratings [5, 6]. The comparison of dependences for the spectrum and output intensity also shows the singularities at critical points for the oscillation intensity. No discontinuity is observed in the oscillation intensity, but a pronounced change of derivative dI_3/dr is obvious. In Fig. 2a and b, where the critical value of r is close to the threshold of oscillation, the effect is rather modest but still well detectable: the rate of fall-off of the oscillation intensity with decreasing r becomes smaller below the bifurcation. In Fig. 2e and f the growth rate of the oscillation intensity with decreasing r increases strongly. Finally, in Fig. 2c and d even the change is observed in the sign of the derivative: the oscillation intensity already decreasing with decreasing r starts to grow again below the bifurcation. In practically all cases (shown in Fig. 2 and observed in other experiments) the splitting of the oscillation spectrum is accompanied by a more or less pronounced improvement of the specific oscillation efficiency, i.e. dI_3/dr is decreasing.

It should be noted that the oscillation beam that propagates roughly in the direction of the cavity axis was observed also in the case where the conventional mirror was removed. This proves that parametric mirror-less oscillation can be achieved with reflection gratings, too.

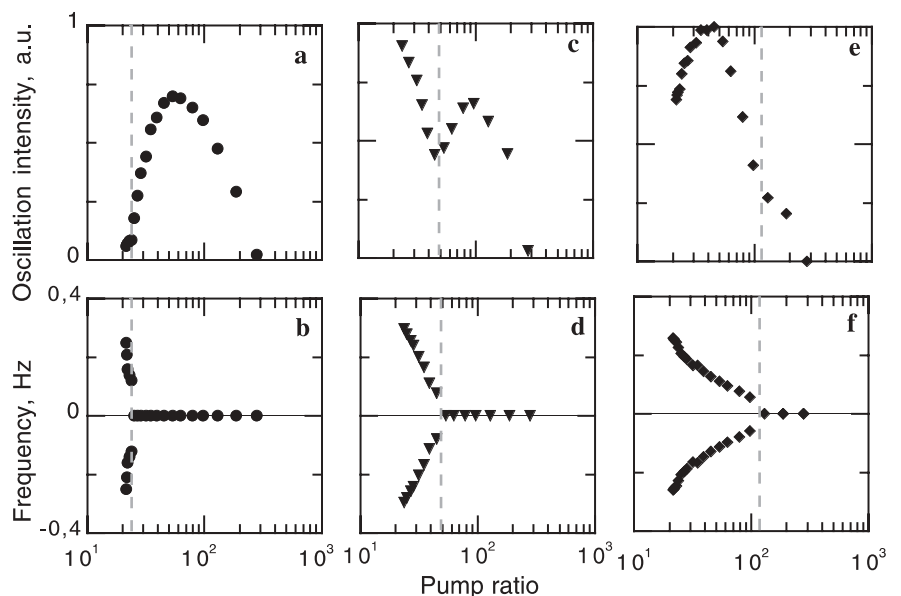


FIGURE 2 Experimentally measured dependences of oscillation intensity (a, c, e) and oscillation spectra (b, d, f) on pump-intensity ratio for coupling strength $\gamma_0\ell \approx -7$

3 Calculations

The oscillation is analysed within the plane-wave approximation with the standard set of equations for slowly varying amplitudes A_i [2]:

$$\begin{aligned} \frac{dA_1}{dz} &= \frac{\gamma}{I_0} (A_1 A_3^* + A_2^* A_4) A_3, \\ \frac{dA_2^*}{dz} &= \frac{\gamma}{I_0} (A_1 A_3^* + A_2^* A_4) A_4^*, \\ \frac{dA_3^*}{dz} &= \frac{\gamma}{I_0} (A_1 A_3^* + A_2^* A_4) A_1^*, \\ \frac{dA_4}{dz} &= \frac{\gamma}{I_0} (A_1 A_3^* + A_2^* A_4) A_2. \end{aligned} \quad (1)$$

The photorefractive crystal itself possesses a purely nonlocal nonlinear response and its coupling constant γ_0 is therefore real; γ becomes complex in the case of nearly degenerate wave mixing, as discussed later.

When written in such a form, ((1)) take into consideration only reflection gratings that couple pump waves to the oscillation waves. Equations ((1)) have no terms responsible for coupling of two counterpropagating pump and/or two counterpropagating oscillation waves because in the experiment these waves are mutually incoherent.

The approach that is used in the present paper differs from [2] in solving ((1)) with the allowance for a small arbitrary frequency shift Ω of the oscillation wave with respect to the fixed frequency of the two pump waves. This implies that the coupling constant of the photorefractive crystal with the diffusion-driven nonlinearity has the complex value

$$\begin{aligned} \gamma\ell &= \frac{\gamma_0\ell}{1 + (\Omega\tau)^2} + i \frac{\Omega\tau\gamma_0\ell}{1 + (\Omega\tau)^2} \\ &= \gamma''\ell + i\gamma'\ell, \end{aligned} \quad (2)$$

where τ is the space-charge decay time. Such an approach makes it possible to predict and study the bifurcation in the oscillation spectrum that occurs at a certain critical value of pump-intensity ratio and then to calculate the oscillation intensity.

It has already been pointed out in [2] that the last two equations of the set ((1)) are identical to those of a set for transmission gratings if the beams are renamed $A_1 \rightarrow A_3 \rightarrow A_2 \rightarrow A_4 \rightarrow A_1$. This leads to the important conclusion that in the undepleted pump approximation (when the first two equations of

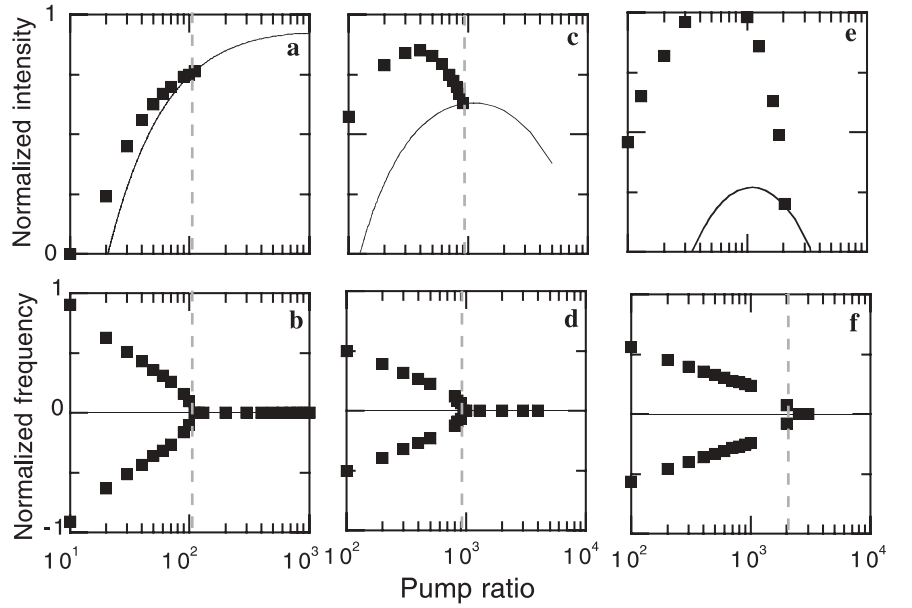


FIGURE 3 Calculated dependences of oscillation intensity (a, c, e) and oscillation spectra (b, d, f) on pump-intensity ratio for coupling strength $\gamma_0\ell \approx -7$ and different reflectivities of the conventional mirror, $R_c = 0.05$ (a, b), 0.01 (c, d), and 0.005 (e, f)

the set ((1)) are reduced to $dA_1/dz = dA_2^*/dz = 0$) all predictions of the theory that was developed for transmission gratings are valid also for wave mixing with reflection gratings.

Therefore, all data for the threshold coupling strength and for oscillation spectra at threshold for the reflection-grating-based oscillator are identical to those for oscillation with the transmission gratings [5, 6].

Furthermore, we consider strong interaction and calculate for the first time the oscillation intensities. Within the range of parameters where frequency-degenerate operation occurs ($\Omega\tau = 0$) the analytical solutions are found for the oscillation intensity by combining the condition for persistent oscillation

$$R \times R_{pc} = 1 \quad (3)$$

and the exact solution for the reflectivity of a phase-conjugate mirror with a $\pi/2$ -shifted reflection grating [2],

$$R_{pc} = \frac{I_1(0)}{I_4(0)} \tanh^2 |g_0| L, \quad (4)$$

where R is the reflectivity of the conventional mirror M_c , $q = I_4(0)/[I_1(0) + I_2(\ell)]$, and $|g_0| L$ can be found from the equation

$$\begin{aligned} \sinh(|g_0| L) &= \frac{\sqrt{(r+1)rq} [1 - \exp(-\gamma\ell)]}{1 + r \exp(-\gamma\ell) + (r+1)q}. \end{aligned} \quad (5)$$

A boundary condition

$$I_4(0) = R I_3(0) \quad (6)$$

gives the relation for the intensities of two oscillation waves counterpropagating inside the cavity.

It follows from ((2))–((4)) that $I_3(0)$ is a solution of

$$\begin{aligned} r^2 R^2 \left(\frac{I_3(0)}{I_2(\ell)} \right)^2 + r R \left(\frac{I_3(0)}{I_2(\ell)} \right) \\ \times (2(1 + r e^{-\gamma_0\ell}) + r(1 - e^{-\gamma_0\ell})^2) \\ + (1 + r e^{-\gamma_0\ell})^2 - r R (1 - e^{-\gamma_0\ell})^2 = 0. \end{aligned} \quad (7)$$

For nondegenerate oscillation the photorefractive coupling constant is a complex value and the numerical simulations have been performed to find the phase-conjugate reflectivity. The frequency shift for any particular pump ratio was imposed to be that found at the threshold, independently of the oscillation intensity. This important assumption was justified by calculation and also experimental results: the frequency detuning was found to change no more than 15% when the coupling strength was increased by 25% from its threshold value.

Figure 3 shows three pairs of calculated pump-ratio dependences $I_3 = I_3(r)$ and $\Omega = \Omega(r)$ for $\gamma_0\ell = -7$ and a reflectivity of the conventional mirror $R = 0.05$ (Fig. 3a and b), 0.01 (Fig. 3c

and d), and 0.005 (Fig. 3e and f), respectively. The value of the coupling strength is chosen to be close to that ensured by the sample used in the experiment, while particular R values are chosen to get dependences qualitatively similar to those experimentally measured (Fig. 2). The solid lines in Fig. 3a, c, and e represent an analytical solution for $\Omega = 0$. In every frame they are valid only above the critical value $r \geq r_{\text{cr}}$ where a bifurcation of the oscillation spectrum occurs. For r below r_{cr} the results of computer simulation are shown as filled squares.

4 Discussion

Let us summarise some general features of the calculated dependences. First of all, the critical value of the pump ratio r_{cr} becomes smaller if cavity losses are decreasing (R becomes higher). This is in agreement with our previous calculations of the oscillation spectra for different R [5, 6].

Also consistent with previous data is the conclusion that bifurcation can occur at r_{cr} , which is larger than the pump ratio that provides maximum output intensity (high cavity losses and mirror-less oscillation with $r_{\text{cr}} \rightarrow \infty$) or smaller than this value (relatively small cavity losses). The behaviour of the oscillation intensity is quite different in these limiting cases. For small losses the

frequency splitting results only in a relatively small extension of the r interval where oscillation occurs and a relatively small change of the derivative dI_3/dr (see Fig. 3a and b). For large cavity losses (see Fig. 3e and f) the changes are more dramatic: with the onset of two-frequency oscillation both the absolute oscillation intensity and the derivative dI_3/dr become much larger than above the bifurcation. By varying the cavity losses it is possible to find the situation where a frequency split occurs near the maximum intensity of the single-frequency oscillation. Here too, the changes in oscillation intensity and in the derivative are very pronounced (see Fig. 3c and d).

Qualitatively, three representative solutions of Fig. 3 correspond to three experimental sets of measurements shown in Fig. 2. A question may arise: do we really meet in the experiment such high cavity losses as for the calculated curves? While it is difficult to believe in high absolute values of losses, minor changes in the lateral position and in the tilt of the 1-mm-long, 0.5-mm cylindrical aperture can strongly affect real values of an effective R . This explains a high sensitivity of oscillation parameters to precise adjustment of pump waves and cavity elements.

To conclude, the simulation procedure used is well justified either for small frequency detunings, $\Omega \rightarrow 0$, and/or for

small oscillation intensities. Nevertheless, it gives reasonable results even beyond these limits, as one can judge from the rather fair qualitative agreement of data presented in Figs. 2 and 3.

ACKNOWLEDGEMENTS The support of the Alexander von Humboldt Foundation via a Research Award attributed to one co-author (S.O.) is gratefully acknowledged.

REFERENCES

- 1 J. Feinberg, R. Hellwarth: *Opt. Lett.* **5**, 519 (1980)
- 2 M. Cronin-Golomb, B. Fisher, J.O. White, A. Yariv: *IEEE J. Quantum Electron.* **QE-20**, 12 (1984)
- 3 D.A. Rockwell: 'Application of Phase Conjugation to High Power Lasers'. In: *Optical Phase Conjugation*, ed. by M. Grower, P. Proch (Springer, Berlin, Heidelberg 1994) p. 228
- 4 S.R. Liu, G. Indebetouw: *J. Opt. Soc. Am. B* **9**, 1507 (1992)
- 5 P. Mathey, S. Odoulov, D. Rytz: *Phys. Rev. Lett.* **89**, 053901 (2002)
- 6 P. Mathey, S. Odoulov, D. Rytz: *J. Opt. Soc. Am. B* **19**, 2967 (2002)
- 7 P. Mathey, P. Jullien, S. Odoulov, O. Shynkarenko: *Appl. Phys. B* **73**, 711 (2001)
- 8 P. Mathey, P. Jullien, S. Odoulov, O. Shynkarenko: *J. Opt. Soc. Am. B* **19**, 405 (2002)
- 9 G. Valley: *J. Opt. Soc. Am. B* **4**, 14 (1987); erratum *J. Opt. Soc. Am. B* **4**, 934 (1987)
- 10 V.A. D'yakov, S.A. Korol'kov, A.V. Mamaev, V.V. Shkunov, A.A. Zozulya: *Opt. Lett.* **16**, 1614 (1991)
- 11 T. Honda, T. Yamashita, H. Matsumoto: *Opt. Commun.* **103**, 434 (1993)
- 12 T. Honda, H. Matsumoto: *J. Opt. Soc. Am. B* **11**, 1983 (1994)